

https://doi.org/10.1070/QEL17265

Influence of growth temperature of $KTiOAsO_4$ single crystals on their physicochemical parameters and formation of domain structures

L.I. Isaenko, A.P. Eliseev, D.B. Kolker, V.N. Vedenyapin, S.A. Zhurkov, E.Yu. Erushin, N.Yu. Kostyukova, A.A. Boiko, V.Ya. Shur, A.R. Akhmatkhanov, M.A. Chuvakova

Abstract. **A potassium titanyl arsenate ($KTiOAsO_4$, KTA) crystal $50 \times 80 \times 60$ mm in size has been grown by upgraded Czochralski method from flux (TGGS) with a decrease in temperature from 900 to 770 °C during pulling. It is shown that the spectroscopic properties of the parts of KTA crystals grown at 900 and 770 °C are close, whereas the electrical conductivity of the low-temperature (770 °C) KTA part turned out to be an order of magnitude lower than that of the high-temperature part. Visualisation of the domain structure by second-harmonic generation microscopy revealed a more efficient domain intergrowth (throughout the sample) in the low-temperature KTA, which is important for forming a regular domain structure (RDS) in a KTA-based nonlinear optical element. It is established that the quantum efficiency of parametric generation of light in the RDS formed in low-temperature KTA is several times higher than in the case of high-temperature KTA. The results obtained are important for optimising RDS parameters.**

Keywords: *potassium arsenate titanyl crystal, absorption spectra, regular domain structures, parametric generation of light.*

1. Introduction

Domain engineering in nonlinear optical ferroelectric crystals [1] allows one to use the quasi-phase-matching (QPM) method to implement second-order nonlinear effects. The nonlinear optical coefficient can be periodically modulated due to the formation of crystals with a regular domain structure (RDS) [2, 3].

The IR spectral range of application of optical parametric oscillators based on potassium titanyl phosphate crystals ($KTiOPO_4$, KTP) is limited by 3.2 μm, whereas the expansion of the spectral range of lasing frequencies is one of important problems of nonlinear optics. Using potassium titanyl arsenate ($KTiOAsO_4$, KTA) crystals with a RDS, one can improve the parameters of optical parametric oscillators (OPOs) in the IR range. Advantages of KTA in comparison with KTP are lower absorption in the visible range [4, 5], a wider transparency range in the mid-IR region (up to 5.2 μm) [6–8], and higher nonlinear susceptibility [9, 10]. The optical damage threshold of KTA crystals pumped by pulsed Nd:YAG laser radiation with a wavelength of 1.064 μm and pulse duration of 8 ns is about 1.2 GW cm^{-2} [8], which is an order of magnitude larger than for periodically polarised MgO:LN crystals and twice as large as for KTP. These properties of KTA crystals have already made it possible to implement high-efficiency OPOs [9], as well as high-efficiency difference-frequency generators and second-harmonic generators with continuous pumping [4, 5].

KTP crystals are known to have cationic conductivity, which is 8 to 10 orders of magnitude higher than the ionic conductivity of lithium niobate (LN); this circumstance hinders the RDS formation in these crystals at room temperature [5, 9]. A decrease in temperature from room to 170 K reduces the electrical conductivity by five orders of magnitude [11]. Moreover, KTP crystals grown in a gradient temperature field may have fairly low electrical conductivity, which allows for their efficient application in electro-optics [12]. However, a high-efficiency KTP-based OPO was designed only with RDS formed in cryogenic temperatures [13].

In situ registration of domain kinetics with a high temporal resolution in the case of polarisation switching in a homogeneous electrical field in KTA crystals [14] made it possible to reveal the main stages of domain structure evolution and measure the velocities of domain walls of different types. The hatching stage (spontaneous formation and growth of quasi-regular ensembles of parallel narrow stripe domains) was revealed for the first time. Measurements of the field dependences of velocities of fast and slow domain walls made it possible to estimate their mobilities and threshold fields. It was found that the ratio of the mobilities of the domain walls parallel to the (110) crystallographic plane and the walls parallel to the (100) plane in KTA is larger than the corresponding ratio for KTP by a factor of 6. The anomalously high mobility ratio facilitates the formation of periodic domain structures and suppresses undesirable expansion of stripe domains, which makes KTA crystals very attractive for RDS fabrication.

The purpose of this work was to study the spectroscopic properties and electrical conductivity of KTA crystals and fabricate RDS's in KTA single crystals grown at different temperatures and to show how the quality of RDS srtuctures

L.I. Isaenko, A.P. Eliseev, V.N. Vedenyapin Novosibirsk National Research State University, ul. Pirogova 1, 630090 Novosibirsk, Russia;
D.B. Kolker, N.Yu. Kostyukova, A.A. Boiko Novosibirsk National Research State University, ul. Pirogova 1, 630090 Novosibirsk, Russia; Novosibirsk State Technical University, prosp. Karla Marksa 20, 630073 Novosibirsk, Russia; Institute of Laser Physics, Siberian Branch, Russian Academy of Sciences, prosp. Akad. Lavrent'eva 15B, Novosibirsk, 630090 Russia; e-mail: dkolker@mail.ru;
S.A. Zhurkov Sobolev Institute of Geology and Mineralogy, Siberian Branch, Russian Academy of Sciences, prosp. Akad. Koptyuga 3, 630090 Novosibirsk, Russia;
E.Yu. Erushin Novosibirsk State Technical University, prosp. Karla Marksa 20, 630073 Novosibirsk, Russia;
V.Ya. Shur, A.R. Akhmatkhanov, M.A. Chuvakova Ural Federal University named after the first President of Russia B.N. Yeltsin, ul. Mira 19, Yekaterinburg, 620002 Russia

Received 9 February 2020; revision received 14 May 2020
Kvantovaya Elektronika **50** (8) 788–792 (2020)
Translated by Yu.P. Sin'kov

depends on the growth temperature. A comparative analysis of the RDS's in KTA crystals as nonlinear OPO elements was performed. The dependences of idler wave energy on the pump energy were investigated, the OPO thresholds and quantum and differential efficiencies of OPOs with RDS's having different periods were determined, and the spectra of the signal wave for OPOs based on different RDS's in KTA were measured.

2. Experimental

KTA single crystals were grown from flux using an upgraded Czochralski method (top-seeded solution growth, TSSG). The growth technique was described in detail in [15]. A KTA crystal of high optical quality, more than 60 mm long and more than 80 mm in diameter, was grown from flux (using $K_6As_4O_{13}$ as a solvent) on a seed oriented along the [100] direction, with gradual decrease in temperature from 900 to 770 °C and simultaneous pulling (with weight control) at a rate from 1 to 2 mm per day. In the initial growth stage the crystal was formed at a temperature of about 900 °C; in the final stage, the bottom part of the crystal was formed at about 770 °C. The single-crystal KTA boule is shown in Fig. 1.

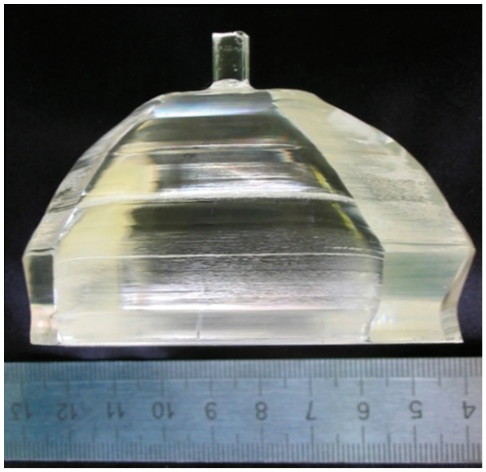

Figure 1. Single-crystal KTA boule more than 40 mm in height and more than 80 mm in diameter.

The determination of crystal transparency range is important for both the investigation and development of various optical devices [7]. The transmission spectra of crystals were measured in the visible and near-IR regions using a UV-2501PC spectrometer (Shimadzu, Japan). Mid-IR transmission spectra were recorded on an IR Fourier spectrometer FT-801 with a microattachment (Simeks, Novosibirsk).

Electrical measurements of samples were performed using a Plexiglas cell. A sample was clamped between two silicone rings. Electrolyte (saturated LiCl aqueous solution) was poured into the cavity formed and closed from above by Plexiglas plates with silicone seal spacers. The cell had channels to supply voltage to the liquid electrode. The current through the sample was determined from the voltage drop on a successively connected precise measuring resistor (0.2, 2, 20, or 200 kΩ, depending on the chosen current measurement limit; the voltage was supplied (through an operational amplifier voltage follower) to an ADC of PCI-6251 board. To measure conductivity, rectangular pulses of external electric field with an amplitude of 2 kV mm^{-1} were applied to sample. The applied field magnitude was smaller than that necessary for polarisation switching; therefore, the chain current was related to only the sample conductivity. The sample conductivity was calculated from the current value j_m, averaged over a time interval of 0.5 s:

$$\sigma = j_m L/(US), \quad (1)$$

where U is the applied voltage, L is the sample thickness, and S is the electrode area.

An RDS was formed in KTA crystals by applying an electric field through an array of stripe electrodes, formed by photolithography. A saturated LiCl aqueous solution, deposited on a periodic array of stripe windows in a photoresist layer [1], was used as an electrode. The array of stripe electrodes was a set of individual 'tracks' with periods of 39.2–45.2 μm. The RDS formed in the sample bulk was visualised by second-harmonic generation microscopy [1].

3. Optical parametric oscillators

A schematic of the experimental setup of the OPO is presented in Fig. 2. The OPO pump source was a TECH-1053 Advanced Nd:YLF laser (Laser-export, Russia) with a wavelength of 1053 nm and pulse duration of 8 ns; the laser pulse repetition rate was varied from 0.02 to 4 kHz, and the maximum pulse energy was about 1 mJ. The pump laser linewidth was 1 cm^{-1}, the beam quality factor was $M^2 < 1.3$, and the half-divergence angle was ~1.8 mrad.

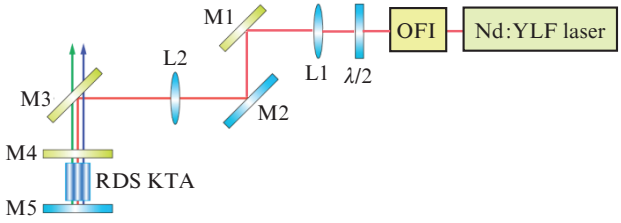

Figure 2. Schematic of the experimental setup: (OFI) optical Faraday isolator; (λ/2) half-wave plate; (L1) lens (f = 300 mm); (L2) lens (f = 174 mm); (M1, M3, M4) dichroic mirrors; (M2, M5) metal mirrors.

By using mirrors M1 and M3 [highly reflective (HR) at 1053–1064 nm, highly transmissive (HT) at 1140–1630 nm, and HT at 3000–14000 nm] and silver mirror M2, mounted on a movable carriage, the pump beam was introduced into the OPO cavity. The cavity was formed by mirrors M4 (HT at 1053–1064 nm, HR at 1310–1470 nm, HT at 3000–6000 nm), M5 (Ag mirror), and the RDS formed in KTA. The pump beam waist necessary for achieving the OPO threshold in the periodically poled KTA (PPKTA) crystal with a diameter d = 480 μm was formed using lens L1 (CaF_2) with a focal length of 300 mm and fused silica lens L2 with a focal length of 174 mm.

All experiments were performed under conventional conditions, without photostabilising the temperature of PPKTA. To minimise the signal wave losses, a single-layer antireflection coating was deposited on the faces of the PPKTA struc-

ture. The spectra of the signal wave were recorded on an NIR-512 spectrometer (Ocean Optics).

4. Experimental results and discussion

Figure 3 shows the transmission spectra of KTA from UV to mid-IR. It can be seen that the KTA transparency range is 0.35–5.2 μm (for KTP, this range is from 0.35 to 3.2 μm), which is in agreement with the data in the literature [16, 17]. It is accepted to explain the expansion of KTA transparency range in comparison with that of KTP by the replacement of phosphorus atoms with larger arsenic atoms.

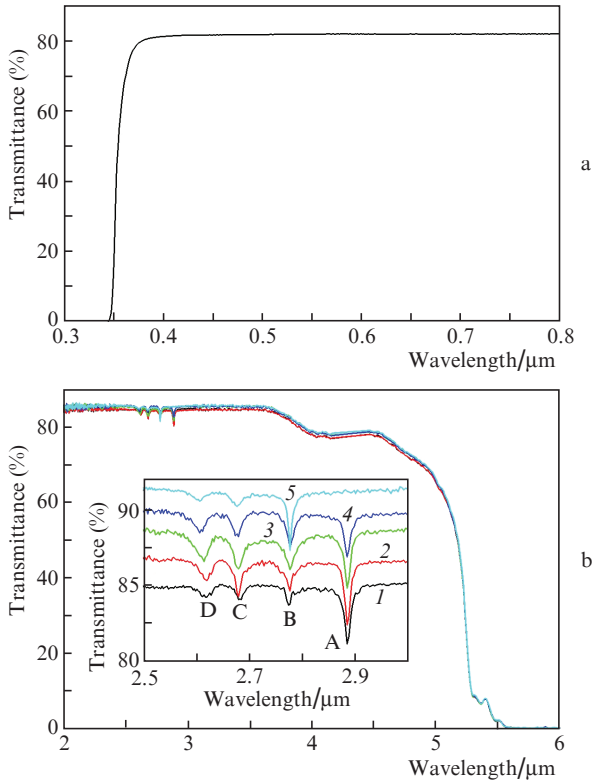

Figure 3. Transmission spectra, measured at room temperature at five points along a 2-mm-thick KTA plate in the (a) UV, visible, and near-IR ranges and (b) mid-IR range. The inset shows a fragment of the transmission spectrum in the vicinity of 2.8 μm. Spectra *1*–*5*, corresponding to different crystal growth temperatures, are shifted along the vertical axis.

A plate (001), 2 mm wide and 40 mm long, was cut from a KTA crystal along its growth direction (*x* axis), and then transmission spectra were recorded through polished faces (001) at five points. The first measurement corresponded to the crystal region formed in the initial growth stage at a temperature of about 900 °C (Fig. 3b, spectrum *1*), and the last measurement corresponded to the final growth stage at 770 °C (Fig. 3b, spectrum *5*). Spectra *2*–*4* were recorded at some intermediate temperatures. It can be seen that, on the whole, the transmission spectrum depends weakly on temperature. It contains a plateau in the range of 0.4–3.6 μm. In the range of 2.5–3.0 μm, there are four narrow and rather weak absorption lines: line A at 2.887 μm (wave number 3463 cm^{-1}), line B at 2.778 μm (3599 cm^{-1}), line C at 2.681 μm (3729 cm^{-1}), and line D at 2.615 μm (3824 cm^{-1}); in the inset of Fig. 3b, these four lines are shown on an enlarged scale. Absorption lines near 2.8 μm were also observed previously in the transmission spectra of LN [18], KTP, and isomorphic compounds [7]. It is agreed that these lines are due to the absorption on defects that are induced by protons captured in the lattice and bound with certain oxygen atoms. A proton–oxygen pair oscillates as a hydroxyl molecule and, therefore, manifests itself as an OH^- defect [19]. These bands are interpreted as stretching vibrations in the OH^- group (mode ν_3 near 2.8 μm) [19]. One line is generally observed for a certain OH^- centre in the LN spectrum [18]. The presence of four spectral lines (A, B, C, and D) indicates that a proton in the KTA crystal forms complexes with four different oxygen atoms.

Figure 4 shows the optical absorption coefficients (calculated from the transmission spectra) in the A, B, C, and D lines for five points on the KTA plate. One can see that there is not any correlation between the lines. All four lines are present in the spectra from the plate parts grown at high temperatures (900 °C and lower); however, with a decrease in temperature to 770 °C, the absorption coefficient for line A gradually decreases, whereas the absorption for line B increases and becomes dominant. The absorption for lines C and D first increases; then passes through a maximum; and, finally, decreases; however, the lines are retained even at $T \approx$ 770 °C.

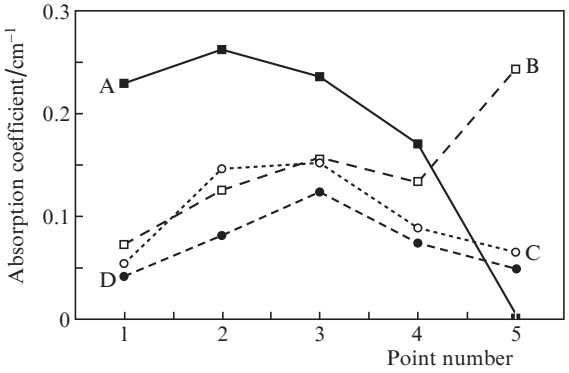

Figure 4. Absorption coefficients for lines A, B, C, and D at different points of KTA plate.

The shape of the absorption spectra of crystals (for example, KTP) is known to depend strongly on the quality of the initial raw material, as well as on the crystal-growth and post-growth treatment conditions [7, 16]. One might suggest that the C and D lines are due to defects with similar structure, whereas hydroxyl complexes, corresponding to the A and B lines, differ significantly in the formation conditions and stability.

The change in the ratio of numbers of K and P ions during KTP crystal growth was studied (using a similar scheme) in [20–22]. It was found that there is some deficit of K ions in the lattice at high temperature, but the composition approaches stoichiometric with a decrease in temperature. We believe a similar pattern to occur during KTA crystal growth; this is a possible explanation of the difference between the absorption spectra of high- and low-temperature parts of crystal.

Two plates were cut from the KTA boule for further studies: one from the lower part, grown at a low (about 770 °C) temperature, and the other from the upper part, grown at an elevated (900 °C) temperature. The plate sizes (*x*, *y*, *z*) were

11.5, 7.5, and 1.15 mm, respectively. When an OPO was designed based on an RDS-containing KTA crystal, the pump beam direction was determined by the angles $\theta = 90°$ and $\varphi = 0$.

The conductivity of the high-temperature sample was 5×10^{-10} Ω^{-1} cm^{-1}, which an order of magnitude higher than that of the low-temperature sample (4×10^{-11} Ω^{-1} cm^{-1}). One might suggest that the KTA conductivity is determined to a great extent by the hydroxyl complexes responsible for the A line in the absorption spectra: the concentration of the corresponding defects is minimal in the KTA crystals grown at about 770 °C (Fig. 4). Note that the conductivity of the samples obtained is nevertheless lower than the characteristic conductivity values for KTP crystals (from 10^{-6} to 10^{-8} Ω^{-1} cm^{-1}) [1].

The choice of optimal parameters of electric-field switching pulse using the previously determined parameters of domain structure kinetics in KTA [14] made it possible to form a homogeneous RDS throughout the entire plate area (Fig. 5).

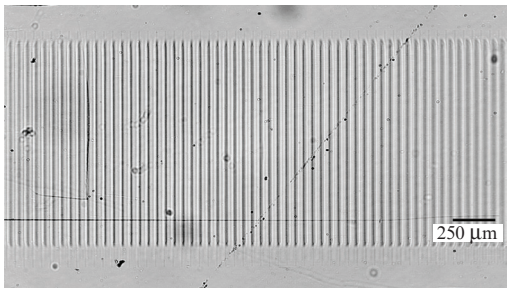

Figure 5. Transmitted-light image of RDS's in a KTA crystal, observed in an optical microscope by the phase contrast method.

The domain structure in the sample bulk was visualised by second-harmonic generation microscopy [1]. It was shown that stripe domains formed in the sample grown at 770 °C are through ones (i.e., extend throughout the entire sample; see Fig. 5), whereas in the sample grown at 900 °C the domains extend to a depth of no more than 800 μm (Fig. 6).

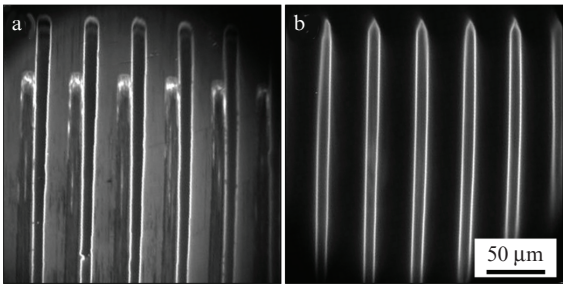

Figure 6. Second-harmonic generation microscopy images of the RDS formed in the high-temperature part of KTA crystal: (a) on the sample surface and (b) at a depth of 600 μm.

We compared the characteristics of PPTKA OPOs corresponding to different growth temperatures. In the first stage of the experiment we investigated the characteristics of a PPTKA OPO with a period of 39.2 μm in the low-temperature KTA sample. Under pumping at λ = 1.053 μm, the signal and idler wavelengths were, respectively, 1.54 and 3.31 μm. The spectra

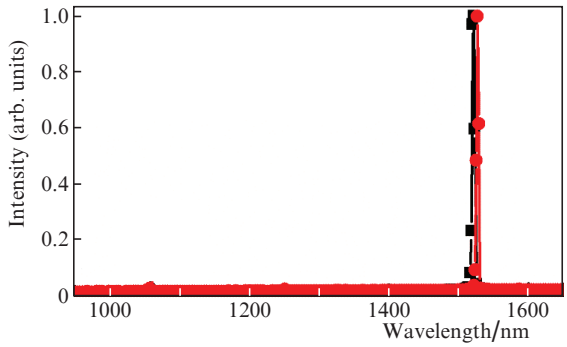

Figure 7. Spectra of OPO signal wave on the (■) second and (●) third tracks (with a period $\Lambda_2 = \Lambda_3 = 39.2$ μm) of RDS in the low-temperature KTA sample.

of the signal wave for two tracks are presented in Fig. 7. It can be seen that they are identical.

Figure 8 shows the dependences of the idler wave energy on pump energy. The parametric generation threshold turned out to be 130 μJ (for a pump intensity of 14.4 MW cm^{-2}), the quantum efficiency was 27%, and the differential efficiency was 12%.

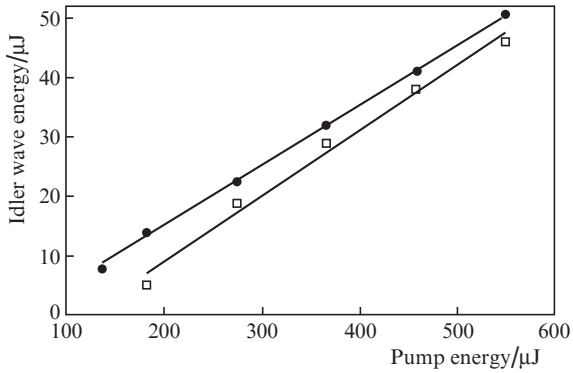

Figure 8. Dependences of the idler wave energy on the pump energy on the second ($\Lambda_2 = 39.2$ μm, ●) and third ($\Lambda_3 = 39.2$ μm, □) RDS tracks in the low-temperature KTA sample; $\lambda_s = 1.54$ μm, $\lambda_i = 3.31$ μm.

In the second stage of the experiment we measured the characteristics of an OPO based on an RDS-containing KTA sample grown at an elevated temperature; the RDS-track periods were $\Lambda_1 = \Lambda_2 = 40.7$ μm and $\Lambda_3 = 39.8$ μm. The following results were obtained: under pumping at $\lambda = 1.053$ μm and for the track period $\Lambda_{1,2} = 40.7$ μm, the signal and idler wavelengths were, respectively, $\lambda_s = 1.698$ μm and $\lambda_i = 2.772$ μm. For a smaller track period ($\Lambda_3 = 39.8$ μm), $\lambda_s = 1.683$ μm and $\lambda_i = 2.813$ μm. The spectra of the signal wave are presented in Fig. 9.

Figure 10 shows the dependences of the idler wave energy on the OPO pump energy at different RDS-track periods in the high-temperature sample. The OPO threshold (track with $\Lambda_1 = 40.7$ μm) amounted to 120 μJ (94.3 MW cm^{-2}), the quantum and differential efficiencies were 12.2 and 7.25%, respectively. For the second track ($\Lambda_2 = 40.7$ μm), the OPO threshold is 172 μJ (135.2 MW cm^{-2}) and the quantum and differential efficiencies are 9.6 and 6.7%, respectively. For the third track ($\Lambda_3 = 39.8$ μm), the corresponding values are 190 μJ (149 MW cm^{-2}), 9.2%, and 6.4%. Note that the quantum effi-

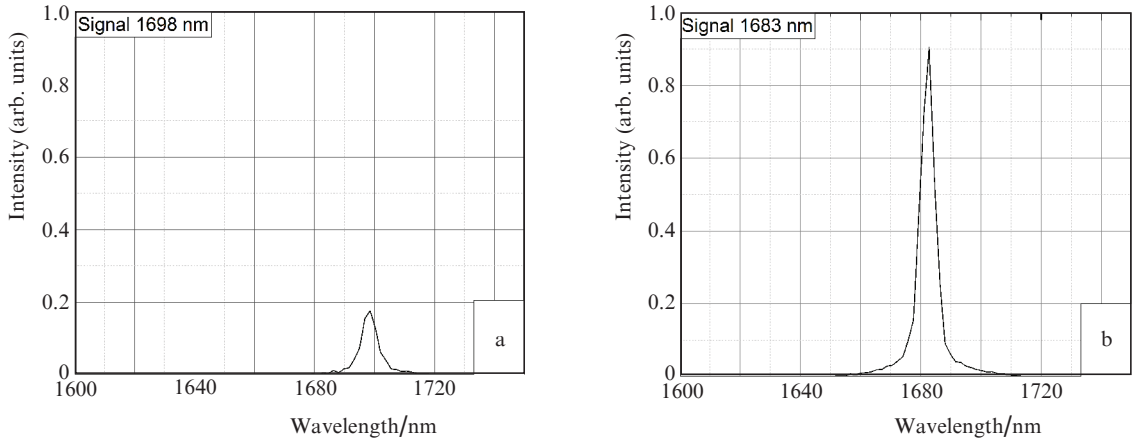

Figure 9. Spectra of OPO signal wave on RDS tracks in the high-temperature KTA sample with periods (a) Λ_1 = 40.7 μm and (b) Λ_3 = 39.8 μm.

ciency of the OPO based on a KTA sample grown at a high temperature turned out to be lower than that of the OPO based on a KTA sample grown at a low temperature.

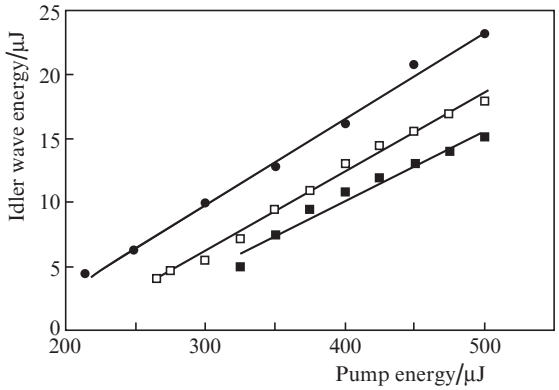

Figure 10. Dependences of the idler wave energy on the pump energy for RDS tracks with periods (●) Λ_1 = 40.7 μm, (□) Λ_2 = 40.7 μm, and (■) Λ_3 = 39.8 μm in the high-temperature KTA sample.

5. Conclusions

A KTA crystal 50 × 80 × 60 mm in size was grown by the TGGS method with a decrease in temperature from 900 to 770 °C during pulling; the upper and lower parts of the crystal were formed at 900 and 770 °C, respectively. The optical characteristics and electrical conductivity of the crystal parts formed at different temperatures were studied. It was noted that the conductivity of the high-temperature part is an order of magnitude higher than that of the low-temperature part.

RDS's were formed in plates cut from the crystal regions grown at 900 and 770 °C. RDS visualisation in the sample bulk by second-harmonic generation microscopy showed that the stripe domains in the sample grown at a temperature of 770 °C are through ones, whereas the domains in the sample grown at 900 °C are extended at a distance of 800 μm from the crystal *Z* face.

It was shown that the quantum efficiency of the OPO based on a low-temperature grown part of the KTA sample is several times higher than that in the OPO based on the high-temperature grown part of the KTA structure.

Acknowledgements. This work was supported by the Russian Science Foundation (Grant No. 19-12-00085) and carried out using equipment of the Ural Centre of Shared Use 'Modern Nanotechnologies' of the Ural Federal University.

References

1. Shur V.Ya., Pelegova E.V., Akhmatkhanov A.R., Baturin I.S. *Ferroelectrics*, **496**, 49 (2016).
2. Byer R.L. *J. Nonlinear Opt. Phys. Mater.*, **6**, 549 (1997).
3. Hum D.S., Fejer M.M. *Comptes Rendus Phys.*, **8**, 180 (2007).
4. Zukauskas A., Pasiskevicius V., Laurell F., Canalias C. *Opt. Mater. Express*, **3**, 1444 (2013).
5. Zeil P., Zukauskas A., Tjörnhammar S., Canalias C., Pasiskevicius V., Laurell F. *Opt. Express*, **21**, 30453 (2013).
6. Cheng L.K., Bierlein J.D. *Ferroelectrics*, **142**, 209 (1993).
7. Hansson G., Karlsson H., et al. *Appl. Opt.*, **39**, 5058 (2000).
8. Nikogosyan D.N. *Nonlinear Optical Crystals. A Complete Survey* (New York: Springer, 2005).
9. Zukauskas A., Thilmann N., Pasiskevicius V., Laurell F., Canalias C. *Appl. Phys. Lett.*, **95**, 191103 (2009).
10. Fradkin-Kashi K., Arie A., Urenski P., Rosenman G. *Opt. Lett.*, **25**, 743 (2000).
11. Rosenman G., Skliar A., Findling Y., Urenski P., Englander A.S., Thomas P.A., Hu Z.W. *J. Phys. D*, **32**, L49 (1999).
12. Nyushkov B.N., Pivtsov V.S., Kolyada N.A., Kaplun A.B., Meshalkin A.B. *Quantum Electron.*, **45**, 486 (2015) [*Kvantovaya Elektron.*, **45**, 486 (2015)].
13. Zhao H., Lima I.T. Jr, Major A. *Laser Phys.*, **20**, 1404 (2010).
14. Akhmatkhanov A.R., Chuvakova M.A., Kipenko I.A., Dolgushin N.A., Kolker D.B., Vedenyapin V.N., Isaenko L.I., Shur V.Ya. *Appl. Phys. Lett.*, **115**, 212901 (2019).
15. Isaenko L.I., Merkulov A.A., Tjurikov V.I., Atuchin V.V., Sokolov L.V., Trukhanov E.M. *J. Cryst. Growth*, **171**, 146 (1997).
16. Bierlein J.D., Vanherzeele H., Ballman A.A. *Appl. Phys. Lett.*, **54**, 783 (1989).
17. Kung A.H. *Opt. Lett.*, **20**, 1107 (1995).
18. Kong Y., Zhang W., Xu J., Yan W., Liu H., Xie X., Li X., Shi L., Zhang G. *Infrared Physics & Technology*, **45**, 281 (2004).
19. Morris P.A., Crawford M.K., Jones B. *J. Appl. Phys.*, **72**, 5371 (1992).
20. Angert N., Tseitlin M., et al. *Appl. Phys. Lett.*, **67** (13), 1941 (1995).
21. Roth M., Angert N., Tseitlin M., Alexandrovski A. *Opt. Mater.*, **16**, 131 (2001).
22. Tu C.-S., Guo A.R., Tao R., Katiyar R.S., Guo R., Bhalla A.S. *J. Appl. Phys.*, **79**, 3235 (1996).